

Revealing the nature of magnetic halos and shadows with radiation MHD simulations

Oskar Steiner^{1,2}, Christian Nutto¹ & Markus Roth¹, ¹Kiepenheuer–Institut für Sonnenphysik, Freiburg, Germany
²Istituto Ricerche Solari, Locarno, Switzerland



What are magnetic halos and shadows?

The *magnetic halo* is an enhancement in the high-frequency (non-trapped) wave power in areas surrounding active regions and network elements both in the photosphere (Brown et al. 1992) and in the chromosphere (Braun et al. 1992; Toner and Labonte 1993) of the Sun. The *magnetic shadow*, on the other hand, is a narrow seam of reduced power surrounding these regions, seen in high-frequency chromospheric intensity and velocity oscillations (Judge et al. 2001; Vecchio et al. 2007b; Kontogiannis et al. 2010a, 2010b; Rajaguru et al. 2012).

Figure 1b shows a *magnetogram* of a field-of-view of 53" x 53" of the solar surface. Figure 1h is the corresponding *power map* of the Doppler velocity of the chromospheric line Ca II 854.2 nm in the frequency range 5.5–8.0 mHz, which samples freely propagating waves above the cutoff period. It shows the *magnetic halo* in the wider surrounding of the magnetic patches and the *magnetic shadow* as a seam of suppressed power in the closer surroundings of the magnetic patches.

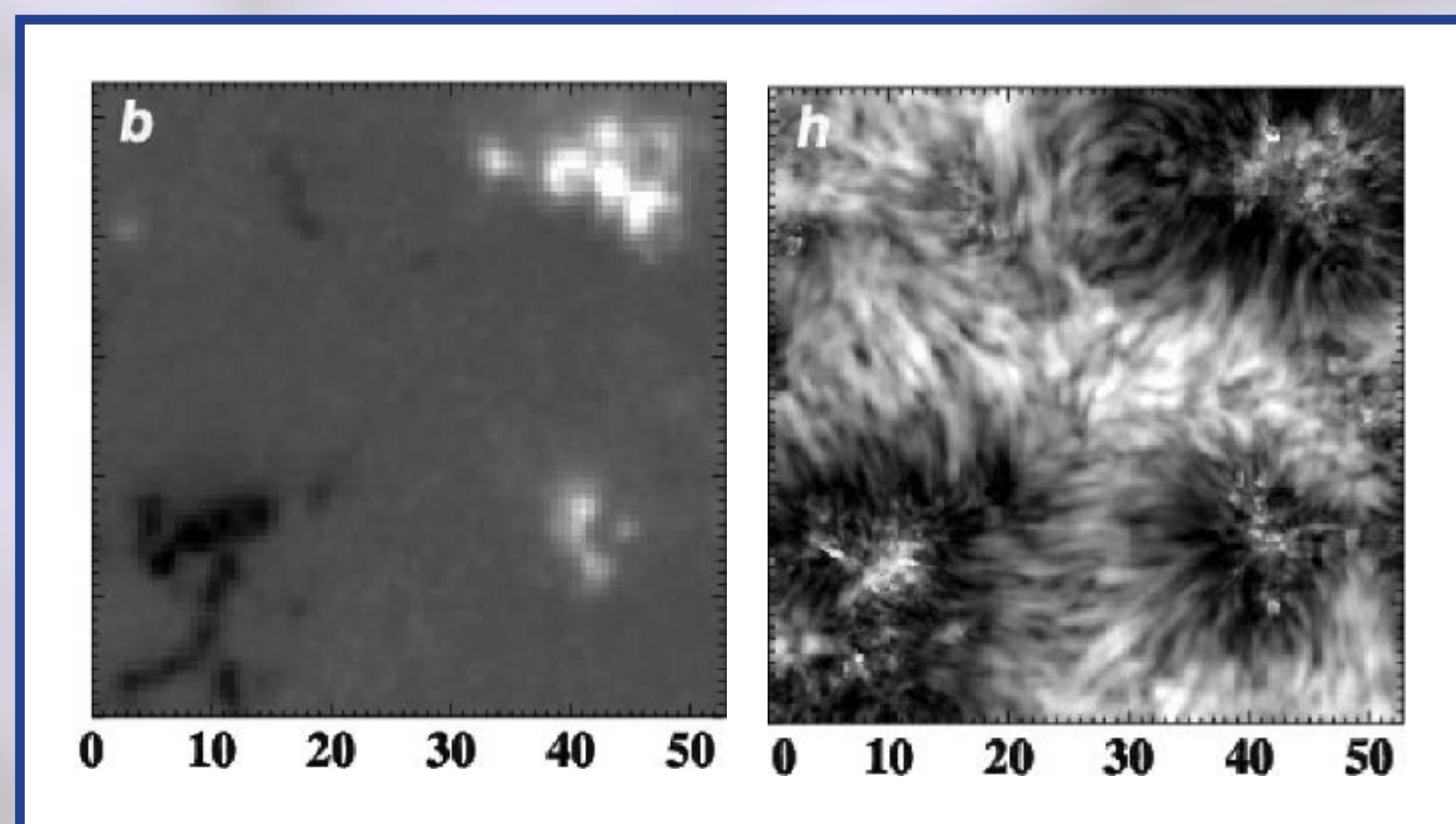


Figure 1: Observations: b) MDI magnetogram of a field-of-view of 53" x 53" of the solar surface. Three magnetic patches (network elements) can readily be seen. h) Power map of the Doppler velocity of the chromospheric line Ca II 854.2 nm in the frequency range 5.5–8.0 mHz. The excess power in the wider surroundings of the magnetic patches is the *magnetic halo*—the lack of power in the closer surroundings is the *magnetic shadow*. Figures from Vecchio et al. (2007).

3-D radiation MHD simulations

We carried out 3-D radiation MHD simulations of the surface layers of the Sun, encompassing a field-of-view of 6" x 6", using the CO⁵BOLD-code (Freytag et al., 2012). An artificial acoustic source, placed at the bottom boundary at a depth of 1.4 Mm below the optical depth $\tau_c = 1$, generates outward traveling, plane parallel, acoustic waves of frequency 10 mHz. Fig. 2, left is a snapshot of the simulation showing the *bolometric intensity*. It displays the typical granular structure of the solar surface. Fig. 2, middle shows the *magnetic field strength* averaged over a time period of 1250 s. Three major patches of magnetic flux concentrations have formed. Fig. 2, right shows the *power map of the vertical velocity perturbation* on an optical depth surface located in the lower chromosphere of the simulation ($\tau_c = 6.7 \times 10^{-5}$). The simulation clearly reproduces the *magnetic shadow* (reduced power in the area between the large and the small ellipses) and the enhanced power of the *magnetic halo* (yellow regions). White contours delineate locations for which sound speed and Alfvén speed are equal.

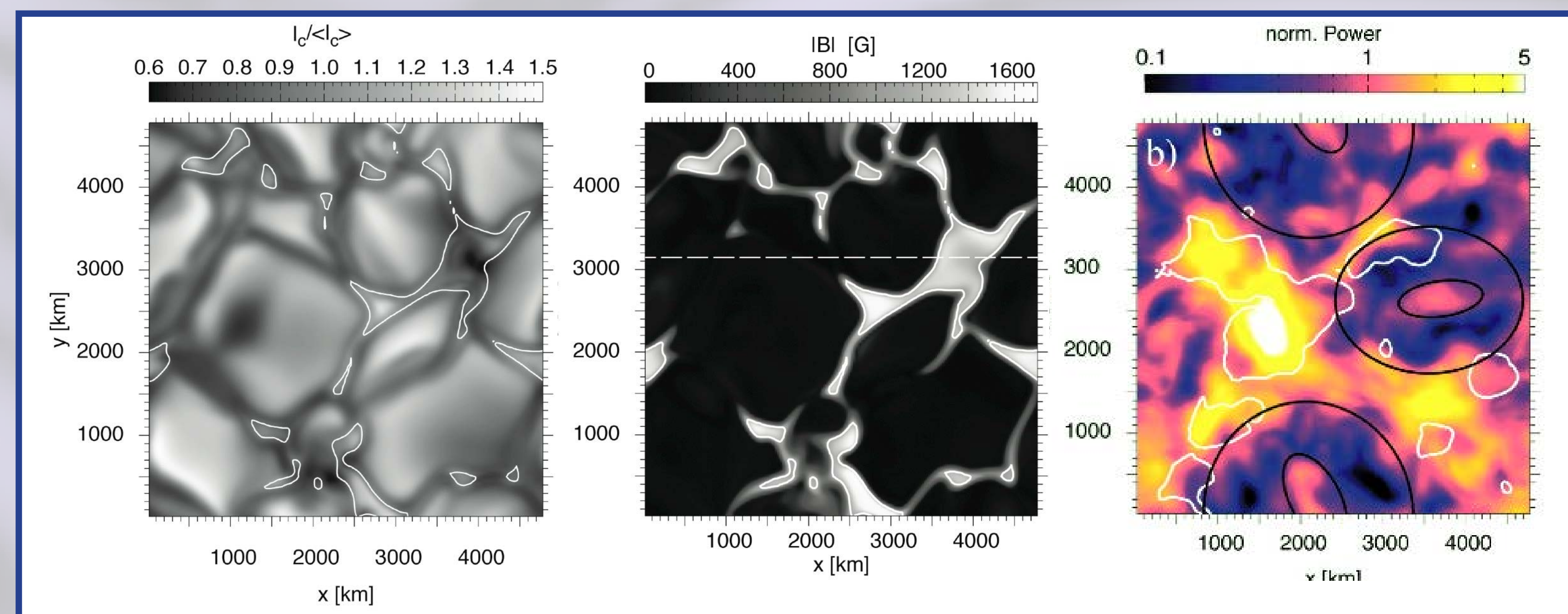
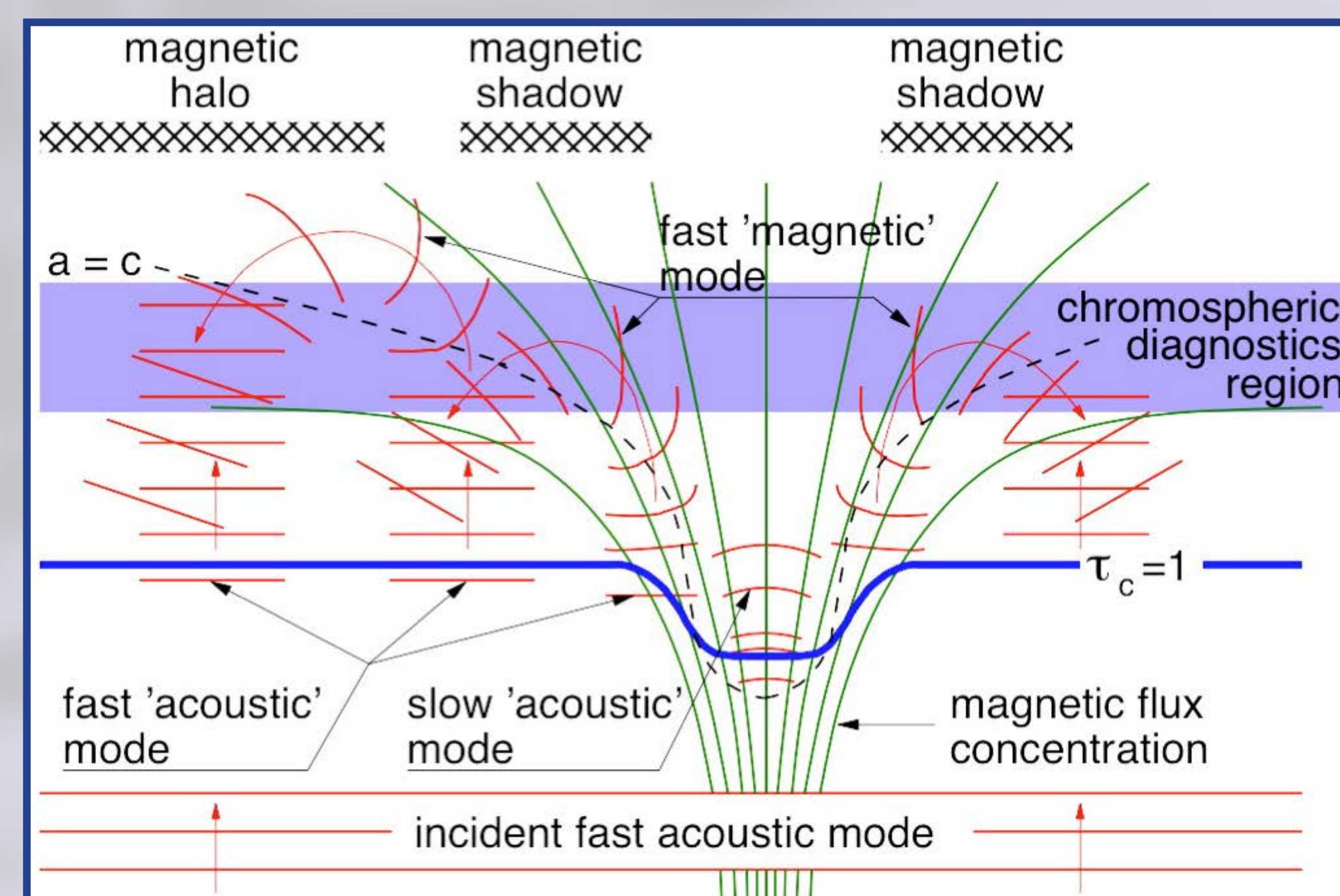


Figure 2: Simulations: Left: Snapshot of the intensity. Granules of the solar surface are visible. White contours localize magnetic fields with a strength of $B_{\text{vert}} \geq 1$ kG. Middle: Time average of the magnetic field strength over 1250 s. Right: Power map of the vertical velocity perturbation, δv_z , in the lower chromosphere. The three inner ellipses mark regions of magnetic flux concentrations. Between the large and the small ellipses, the characteristic annulus of suppressed power of the *magnetic shadow* is apparent. Excess power corresponds to locations of the *magnetic halo*. Adapted from Nutto et al. (2012).

Interpretation

Figure 3 sketches the physics behind the magnetic shadow and halo. In the peripheral region of the magnetic flux concentration (green), acoustic waves enter the region above the dashed curve where the magnetic field dominates the thermal gas pressure (low β , region). There, they convert to *fast, predominantly magnetic waves*, which refract further above because of the steep increase in the Alfvén speed with height. After refraction, the waves travel back into the Sun again, and convert back to acoustic waves. Three such refractive wave paths are indicated in red. The apex of the inner wave train falls into the layers of the employed chromospheric diagnostics (blue band), and because its wave vector is close to horizontal there, the vertical velocity perturbation vanishes and with it the power in the Doppler velocity, hence the *magnetic shadow*. Further out, the downward traveling refracted waves interfere with the continuing incident fast acoustic waves within the diagnostics region, which leads to excess power, hence the *magnetic halo*. In the center of the magnetic flux concentration, the wave vector of the incident acoustic wave is parallel to the magnetic field, which impedes wave conversion, leaving it a *slow, predominantly acoustic wave*, which causes the residual power in the center of the flux concentration, within the small ellipses of Fig. 2, right. Figure from Komm et al. (2013).



References

- Braun, D. C., Lindsey, C., Fan, Y., & Jefferies, S. M.: 1995, Local acoustic diagnostics of the solar interior, *ApJ* 392, 739
- Freytag, B., Steffen, M., Ludwig, H.-G., Wedemeyer-Böhm, S., Schaffenberger, W., & Steiner, O.: 2012, Simulations of stellar convection with CO5BOLD, *J. Comput. Phys.* 231, 919
- Judge, P.G., Tarbell, T.D., & Wilhelm, K.: 2001, A study of chromospheric oscillations using the SOHO and TRACE spacecraft, *ApJ* 554, 424
- Komm, R., De Moortel, I., Fan, Y., Ilonidis, S., & Steiner, O.: 2013, Sub-photosphere to solar atmosphere connection, in Proc. of the ISSI workshop Helioseismology and Dynamics of the Solar Interior, L. Culhane (ed), *Space Sci. Rev.*
- Kontogiannis, I., Tsiropoula, G., & Tziotziou, K.: 2010a, Power halo and magnetic shadow in a solar quiet region observed in the H α line, *A&A* 510, A41
- Kontogiannis, I., Tsiropoula, G., Tziotziou, K., & Georgoulis, M. K.: 2010b, Oscillations in a network region observed in the H α line and their relation to the magnetic field, *A&A* 524, A12
- Nutto, C., Steiner, O., & Roth, M.: 2012, Revealing the nature of magnetic shadows with numerical 3D-MHD simulations, *A&A* 542, L30
- Rajaguru, S. P., Couvidat, S., Sun, X., Hayashi, K., & Schunker, H.: 2012, Properties of High-Frequency Wave Power Halos Around Active Regions: An Analysis of Multi-height Data from HMI and AIA Onboard SDO, *Sol. Phys.* 287, 107
- Toner, C. G. & Labonte, B. J.: 1993, Direct Mapping of Solar Acoustic Power, *ApJ* 415, 847
- Vecchio, A., Cauzzi, G., Reardon, K. P., Janssen, K., & Rimmele, T.: 2007, Solar atmospheric oscillations and the chromospheric magnetic topology, *A&A* 461, L1